Evolution of Magnetic Order from the Localized to the Itinerant Limit

D. G. Mazzone,[1,2,*] N. Gauthier,[3,4,†] D. T. Maimone,[3] R. Yadav,[3] M. Bartkowiak,[3] J. L. Gavilano,[1] S. Raymond,[5] V. Pomjakushin,[1] N. Casati,[6] Z. Revay,[7] G. Lapertot,[8] R. Sibille,[1] and M. Kenzelmann[1]

[1]*Laboratory for Neutron Scattering and Imaging, Paul Scherrer Institut, 5232 Villigen PSI, Switzerland*
[2]*National Synchrotron Light Source II, Brookhaven National Laboratory, Upton, New York 11973, USA*
[3]*Laboratory for Scientific Developments and Novel Materials, Paul Scherrer Institut, 5232 Villigen PSI, Switzerland*
[4]*Stanford Institute for Materials and Energy Sciences, SLAC National Accelerator Laboratory, Menlo Park, California 94025, USA*
[5]*Univ. Grenoble Alpes, CEA, IRIG, MEM, MDN, F-38000 Grenoble, France*
[6]*Swiss Light Source, Paul Scherrer Institut, CH-5232 Villigen PSI, Switzerland*
[7]*Technische Universität München, Heinz Maier-Leibnitz Zentrum, 85747 Garching, Germany*
[8]*Univ. Grenoble Alpes, CEA, IRIG, PHELIQS, IMAPEC, F-38000 Grenoble, France*

(Received 1 February 2019; published 27 August 2019)

Quantum materials that feature magnetic long-range order often reveal complex phase diagrams when localized electrons become mobile. In many materials magnetism is rapidly suppressed as electronic charges dissolve into the conduction band. In materials where magnetism persists, it is unclear how the magnetic properties are affected. Here we study the evolution of the magnetic structure in $Nd_{1-x}Ce_xCoIn_5$ from the localized to the highly itinerant limit. We observe two magnetic ground states inside a heavy-fermion phase that are detached from unconventional superconductivity. The presence of two different magnetic phases provides evidence that increasing charge delocalization affects the magnetic interactions via anisotropic band hybridization.

DOI: 10.1103/PhysRevLett.123.097201

Charge carriers in a periodic array of atoms are found either close to the nuclei or assume a delocalized character where they move freely throughout the crystal. These extreme cases are often well described in the Mott, Kondo, or Fermi liquid theory framework. Materials in intermediate regimes with strong electronic fluctuations are more difficult to describe and can stabilize novel quantum ground states that keep fascinating the condensed matter physics community. Examples include the transition-metal oxides, pnictides, or the heavy-fermion metals [1–4].

In materials with partly delocalized electrons, orbital and spin degrees of freedom can trigger magnetic long-range order. Magnetism is often suppressed by increasing charge delocalization, and it is thought that the associated fluctuations are essential for macroscopically coherent phases such as unconventional superconductivity [1–3]. It is not clear how the magnetic interactions, and the resulting magnetic structure, are modified as the degree of itineracy changes in a material. *Ab initio* calculations are at present not accurate enough to deal with the small energy differences that are relevant, particularly in heavy-fermion metals. In addition, it is an open question how the magnetic interactions are affected in experimental realizations where magnetic order persists over localized-to-itinerant charge transitions [5–7].

Kondo materials are ideal systems to shed light onto this scientific problem. The materials possess energy scales that are up to 4 orders of magnitude smaller than in transition-metal oxides [8], and are, thus, highly susceptible to external tuning parameters, such as magnetic fields or chemical doping [9–11]. The low energy scale arises from partially filled electronic f states that are partly screened by mobile charge carriers. This so-called Kondo coupling can lead to collective singlet states, where localized f electrons admix with the conduction band and become mobile. The development of coherent f bands near the Fermi surface triggers renormalized effective masses below a coherence temperature T_{coh} that allows effectively probing the degree of the system's itinerancy. In addition, heavy-fermion materials can feature localized magnetic order that is in direct competition with Kondo screening, providing an accessible and sensitive measure of the nature of magnetism.

Here, we study the evolution of magnetic properties in $Nd_{1-x}Ce_xCoIn_5$. $CeCoIn_5$ is a highly itinerant heavy-fermion material with a large quasiparticle mass enhancement [12,13]. In contrast, isostructural compounds consisting of Nd ions are known to generate nonhybridized local magnetic moments [14–17]. Previous macroscopic transport measurements have shown that chemical substitution of Nd for Ce in $Nd_{1-x}Ce_xCoIn_5$ allows driving the system from the highly itinerant to the completely localized limit [17]. The series displays zero-field magnetic order for $x < 0.95$ that competes with superconductivity for $x \geq 0.83$, and heavy-electron bands are thought to exist for $x > 0.5$. Hitherto, magnetic order has been explored in detail for $x = 0.95$ only,

where a spin-density wave (SDW) is modulated with $\vec{Q}_{IC} = (q, \pm q, 0.5)$ in reciprocal lattice units (r.l.u.) and $q \approx 0.45$ [18,19]. The ordered magnetic moment, $\mu = 0.13(5)\mu_B$, is aligned along the tetragonal c axis. As we will now show, the magnetic symmetry is modified within the heavy-fermion ground state upon doping, providing evidence for an evolution of the magnetic exchange couplings upon band hybridization.

Single crystalline $Nd_{1-x}Ce_xCoIn_5$ with $x = 0$, 0.16, 0.4, 0.61, 0.75, 0.83, 0.95, and 1 was grown in indium self-flux [12]. The quality of experimental realization with $x = 0$, 0.16, 0.4, 0.61, and 1 was probed via x-ray powder diffraction at the Material Science (MS-X04SA) beam line of the Swiss Light Source at the Paul Scherrer Institut (PSI), Villigen, Switzerland using a photon wavelength $\lambda = 0.56491$ Å [20]. The actual Nd concentration of these samples was determined on the High-Resolution Powder Diffractometer for Thermal Neutrons (HRPT) at the Swiss Neutron Spallation Source (SINQ) at PSI with $\lambda = 1.886$ Å. The Nd concentration in single crystals with $x = 0.95$ was checked by means of in-beam neutron activation analysis at MLZ-Garching, Munich, Germany [21,22]. The macroscopic properties of members with $x = 0$, 0.16, 0.4, 0.61, 0.75, 0.83, and 1 were investigated via four-probe electrical resistivity and ac or dc magnetization measurements in a Quantum Design PPMS or in cryogenic magnets. The macroscopic and microscopic properties of $x = 0.95$ are reported in Ref. [19]. The magnetic structure of $x = 0$, 0.16, 0.4, 0.61 was determined via neutron powder diffraction at HRPT and experimental realizations with $x = 0.75$ and 0.83 were investigated by means of single crystal neutron diffraction on Zebra at SINQ and on the triple-axis spectrometer IN12 at the Institut Laue-Langevin, Grenoble France, respectively. While a neutron wavelength $\lambda = 1.177$ Å was employed on Zebra, $\lambda = 3.307$ and 4.83 Å were used on IN12. All magnetic structures were refined with the FullProf suite [23]. Further detailed information is given in the Supplemental Material [24].

Neutron powder diffraction results on $NdCoIn_5$ are shown in Fig. 1(a) and are representative for $Nd_{1-x}Ce_xCoIn_5$ with $x = 0$, 0.16, 0.4, and 0.61 (see Supplemental Material [24]). We observe magnetic Bragg peaks at low temperatures, consistent with two symmetry-equivalent commensurate propagation vectors $\vec{Q}_C = (1/2, 0, 1/2)$ and $(0, 1/2, 1/2)$. They correspond to different domains that are indistinguishable in a powder diffraction experiment. The evolution of the magnetic Bragg peak intensity at higher scattering angles shows unambiguously that the magnetic moment is oriented along the c axis. We find an Ising-like structure that is displayed in Fig. 1(b) for the $(1/2, 0, 1/2)$ domain.

In contrast, a ground state with incommensurate magnetic order is observed for $x \geq 0.75$. The single crystal neutron diffraction results reveal a magnetic wave vector

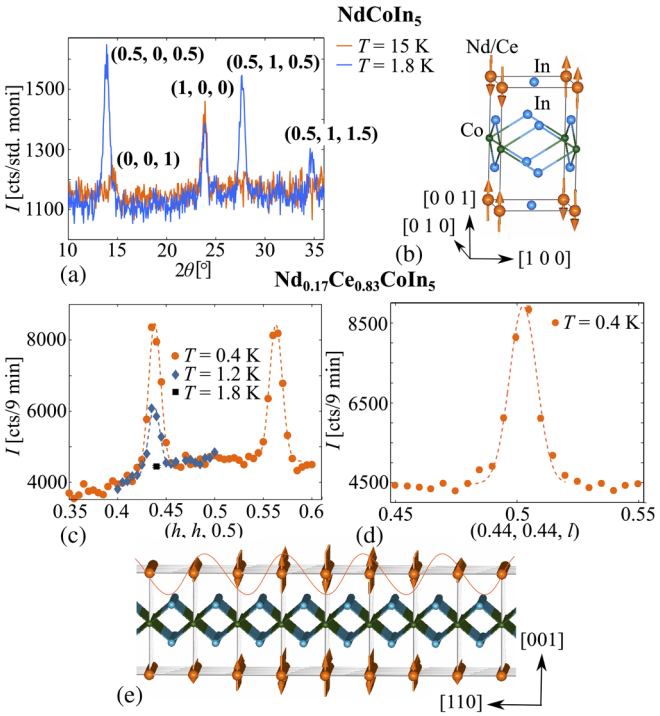

FIG. 1. (a) Neutron powder diffraction results on $NdCoIn_5$ revealing an Ising-like magnetic structure, as shown in (b). Single crystal neutron diffraction intensity of $Nd_{0.17}Ce_{0.83}CoIn_5$ along $(h, h, 0.5)$ in (c) and $(0.44, 0.44, l)$ in (d), given in reciprocal lattice units (r.l.u.). (e) Amplitude modulated magnetic structure, such as observed for $0.75 \leq x \leq 0.95$.

$\vec{Q}_{IC} = (q, \pm q, 0.5)$ with $q \approx 0.44$, for $Nd_{1-x}Ce_xCoIn_5$ with $0.75 \leq x \leq 0.95$ [see Figs. 1(c) and 1(d) for $x = 0.83$ and Supplemental Material [24] for $x = 0.75$]. The propagation vector is similar to the one of $Nd_{0.05}Ce_{0.95}CoIn_5$ [18,19], and the absence of intensity at $\vec{Q}_C$ excludes a scenario where different types of magnetic order coexist. The magnetic moment remains aligned along the tetragonal c axis, but features a sinusoidally modulated structure [see Fig. 1(e)].

The doping dependence of the magnetic moment amplitude is shown in Fig. 2(a). In the commensurate phase, it monotonically decreases from $\mu_p = 2.56(3)\mu_B$ for $NdCoIn_5$ to $0.90(5)\mu_B$ for a Ce concentration of 61%. The modulation direction experiences a rotation in the tetragonal plane and propagates along $\vec{Q}_{IC}$ for $x \geq 0.75$. Here μ_p is modified weakly before it is strongly suppressed for $x > 0.83$. The incommensuration, $q(x)$, increases with increasing Ce content [see Fig. 2(a), inset], which may be attributed to small changes in the Fermi surface. The xT-phase diagram of $Nd_{1-x}Ce_xCoIn_5$ is shown in Fig. 3. The series features persistent magnetism up to $x = 0.95$ that competes with superconductivity at $x \geq 0.83$, and a localized charge state for $x < 0.5$. The key result of our study is that magnetic order is modified between $x = 0.61$ and 0.75, shifted with respect to the onset of coherent heavy bands and superconductivity.

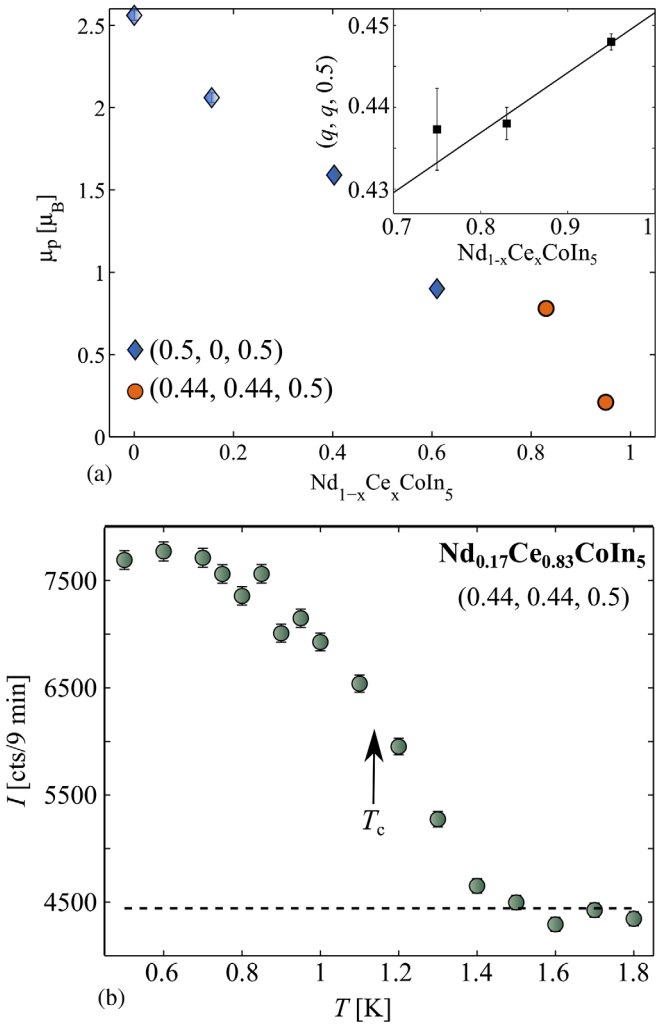

FIG. 2. (a) Evolution of the magnetic moment amplitude as a function of Ce content in $Nd_{1-x}Ce_xCoIn_5$ (the data point at $x = 0.95$ was taken from Ref. [19]). Inset: Incommensuration $(q, q, 0.5)$ as a function of x. (b) Temperature dependence of the magnetic Bragg peak intensity at (0.44, 0.44, 0.5) in $Nd_{0.17}Ce_{0.83}CoIn_5$.

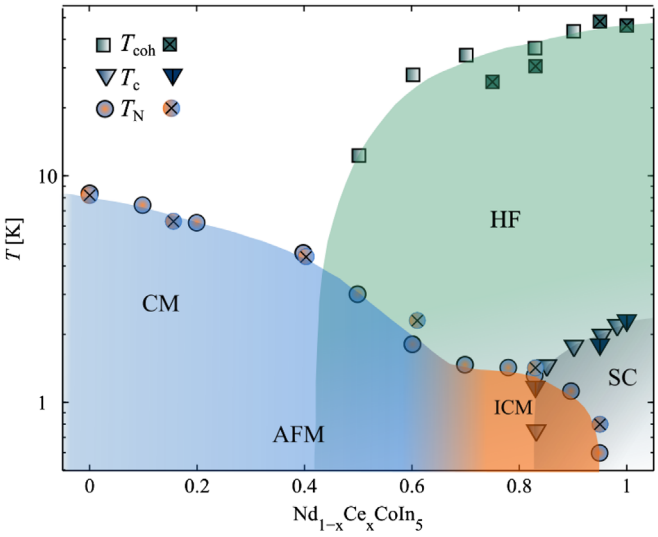

FIG. 3. Antiferromagnetic (AFM) phase for $x \leq 0.95$, superconductivity (SC) for $x \geq 0.83$ and heavy-fermion (HF) properties for $x \geq 0.5$. CM denotes the commensurate structure with $\vec{Q}_C = (1/2, 0, 1/2)$ and $(0, 1/2, 1/2)$. ICM is the incommensurate order along $\vec{Q}_{IC} = (q, \pm q, 0.5)$ with $q \approx 0.44$. Left legend represent data from Ref. [17], the right legend are our data (the phase boundaries of $x = 0.95$ were taken from Ref. [19]).

The superconducting phase at $x > 0.8$ is believed to arise from magnetic fluctuations of a nearby SDW critical point [25]. The Cooper pairs in $CeCoIn_5$ feature $d_{x^2-y^2}$ symmetry that is robust under small Nd substitution [26,27]. The pairing symmetry reveals nodes along the reciprocal (1, 1, 0) direction, where low-energy quasiparticles can mediate magnetic order without directly competing with the condensate. In consequence, the d-wave order parameter is compatible with the incommensurate wave vector $\vec{Q}_{IC}$, but not with $\vec{Q}_C$. This is supported by the temperature dependence of the magnetic Bragg peak intensity in $Nd_{0.17}Ce_{0.83}CoIn_5$ that shows no anomaly as the temperature is tuned across the superconducting phase boundary [see Fig. 2(b)].

The interplay between superconductivity and magnetism observed here is very different from the behavior in isostructural $CeCo_yRh_{1-y}In_5$, where the magnetic moment orientation is altered at the superconducting phase boundary [28–30]. In $Nd_{1-x}Ce_xCoIn_5$ magnetic order along $\vec{Q}_C$ is established between $0.61 < x < 0.75$ where superconductivity is suppressed (see Fig. 3). In contrast, similarities with the xT-phase diagram of the iron-based superconductor $Fe_{1+y}Te_{1-z}Se_z$ are recognized [31]. The material hosts two different types of antiferromagnetic correlations, whose relative weight can be tuned via Se substitution. The dominant correlations at low Se concentrations are associated to weak charge carrier localization that triggers magnetic long-range order. In contrast, antiferromagnetic correlations with a different modulation become important at larger Se concentrations and are thought to be closely related to emergence of superconductivity. Similarly, inelastic neutron scattering studies on $Nd_{1-x}Ce_xCoIn_5$ with $x = 1$ and 0.95 have shown that the magnetic fluctuations related to superconductivity possess a symmetry distinct from the magnetic modulation in the localized limit [32,33]. Thus, an intimate link between magnetic correlations along $\vec{Q}_{IC}$ and $d_{x^2-y^2}$-wave superconductivity is expected in $Nd_{1-x}Ce_xCoIn_5$.

A change of magnetic correlations points towards a doping dependent evolution of the magnetic interactions that is related to the degree of electron mobility. This is observed, for instance, in some layered transition-metal oxides, as they establish a charge- and spin-stripe order that allows accommodating coexisting local antiferromagnetic spin correlations and itinerant charge carriers [34]. In

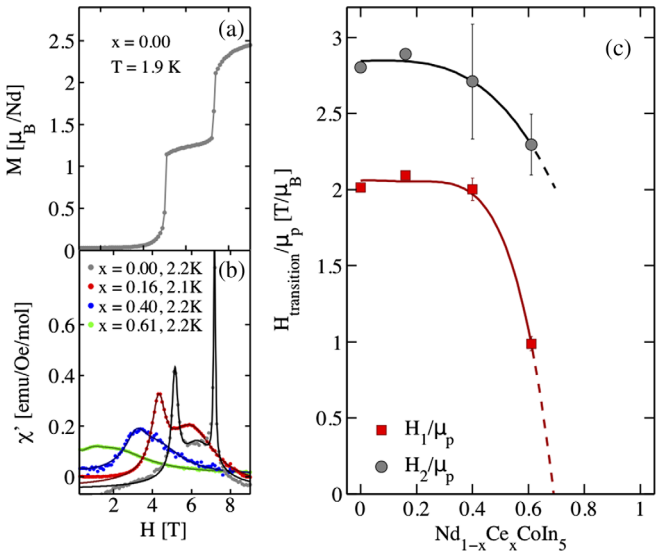

FIG. 4. (a) Field dependent dc magnetization, M, of $NdCoIn_5$ and (b) real part of the ac magnetic susceptibility, χ' in $Nd_{1-x}Ce_xCoIn_5$ with $x = 0$, 0.16, 0.4 and 0.61 for $\vec{H}||[0\,0\,1]$ and $T < T_N$. The two transitions correspond to a spin-flip (H_1) and a ferromagnetic transition (H_2). (c) Field dependence of the two critical fields, $H_{1,2}$, normalized by the ordered moment, μ_p. The solid lines are guides to the eye.

$La_{2-y}Ba_yCuO_4$, for instance, the antiferromagnetic Mott-ground state is suppressed for $y \geq 0.05$, but the inclusion of mobile hole carriers affects the magnetic exchange couplings stabilizing a stripe order. This ground state competes with superconductivity that is also present for $y \geq 0.05$, causing a profound reduction of the critical temperature around $y \approx 1/8$. Similarly, the magnetic interactions in $Nd_{1-x}Ce_xCoIn_5$ may evolve with increasing Ce concentration, and trigger a transition from localized $\vec{Q}_C$ to itinerant $\vec{Q}_{IC}$.

The scenario is further clarified by a comparison with isostructural localized-moment magnets that also show a commensurate structure along $\vec{Q}_C$ [14–16]. The materials feature magnetic order that can be described using an Ising-type Hamiltonian with antiferromagnetic nearest-, next-nearest-neighbor, and an interlayer exchange coupling [16]. Field dependent magnetization and susceptibility measurements inside the antiferromagnetic phase for fields along the tetragonal c axis can reveal valuable information about the exchange couplings. They show two critical fields, $H_{1,2}$, and a plateau region with increasing magnetic field. The ratio of $H_{1,2}$ and the ordered moment, μ_p, is directly related to the magnetic exchange couplings [16]. Similar measurements on $Nd_{1-x}Ce_xCoIn_5$ with $x = 0$, 0.16, 0.4 and 0.6 are shown in Figs. 4(a) and 4(b) and the doping dependence of $H_{1,2}/\mu_p$ is displayed in Fig. 4(c). These results reveal a significant change of the magnetic interactions for $x > 0.5$, coinciding with the onset of the heavy-fermion ground state where localized f electrons become mobile via hybridization with the conduction band.

The underlying microscopic process of the heavy-fermion ground state is driven through collective screening of the conduction electrons, minimizing the total angular momentum of the local $4f$ moments. While this is favorable for Ce ions (Ce^{3+}, $J = 5/2 \rightarrow Ce^{4+}$, $J = 0$), Nd^{3+} remains in a stable $J = 9/2$ configuration. Such a case can be described best using a phenomenological two-fluid model, in which two coexisting contributions of either f electrons that are hybridized at low temperatures or residual local moments are assumed [13,35,36]. Since the Ce-$4f$ ground state wave function in this family of compounds is hybridized mainly with In-p orbitals [37–39], it is conceivable that the antiferromagnetic nearest-, next-nearest-neighbor, and interlayer exchange coupling are affected differently as band hybridization becomes stronger with increasing Ce concentration [see Fig. 1(b)]. This scenario can naturally explain a change in magnetic symmetry inside the heavy-fermion ground state, as opposed to a case where all interactions change on an equal footing.

It is noted that the evolution of the hybridized $4f$-wave function in doped $CeCoIn_5$ strongly depends on the chemical element that is substituted. While Ce substitution simply yields a decrease in the fluid accounting for hybridized f electrons, doping at the other chemical sites has a more complex impact on the electronic ground state [37–40]. It has been shown, for instance, that substitution of the transition metal affects the shape of the Ce-$4f$ ground state wave function [39]. Upon increasing Rh doping the $4f$ orbital is squeezed into the tetragonal basal plane, mainly decreasing the hybridization with the out-of-plane In-p orbitals. This drives the system away from the superconducting ground state and into different magnetic phases [28–30]. Substitution on the In site can also affect the shape of the Ce-$4f$ ground state wave function, but a recent study has shown that it remains unchanged under Cd substitution [40]. In this compound, magnetic order is thought to arise via a local nucleation process, without altering the global electronic structure [41].

A similar controversy has also arisen lately for magnetic order in $Nd_{1-x}Ce_xCoIn_5$ at small x [42–45]. De Haas-van Alphen effect measurements on $Nd_{1-x}Ce_xCoIn_5$, predictions on the behavior of the static spin susceptibility upon (non-)magnetic substitution of Ce in $CeCoIn_5$, and the observation of magnetic order in 5% Gd-doped $CeCoIn_5$ suggest that magnetic order is triggered by an instability in the band structure [42,43]. In contrast, some theoretical models argue that local magnetic droplets play a decisive role [44,45]. In this scenario magnetism is mediated inside a d-wave superconducting background via strong magnetic fluctuations triggered by the nearby SDW critical point. Since we find that magnetic order along $\vec{Q}_{IC}$ persists down to $x = 0.75$ that is both, outside the superconducting dome and far from the SDW critical point, our results are in line with a nonlocal picture involving the Fermi surface topology.

In summary, we report the evolution of magnetism in the series $Nd_{1-x}Ce_xCoIn_5$ from the localized ($x = 0$) to the highly itinerant limit ($x = 1$). We observe two different magnetic structures with moments along the tetragonal c axis. Magnetic order is Ising-like with $\vec{Q}_C = (1/2, 0, 1/2)$ and $(0, 1/2, 1/2)$ for materials with $x \leq 0.61$, and amplitude modulated with $\vec{Q}_{IC} = (q, \pm q, 0.5)$ with $q \approx 0.44$ for $x \geq 0.75$. We find that delocalization of Ce-4f electrons at $x > 0.5$ affects the magnetic interactions, providing evidence for anisotropic hybridization effects. Increasing charge itinerancy leads to a magnetic transition between $x = 0.61$ and 0.75. This occurs far away from the emergence of unconventional superconductivity and is thus unrelated. Our results demonstrate that the magnetic interactions strongly depend on the degree of 4f-electron hybridization with the conduction electrons. This emphasizes the need to include hybridization dependent magnetic interaction in theories describing quantum materials close to the Kondo breakdown, and offers new perspectives for the interpretation of the physical properties in heavy-fermion materials.

We thank the Paul Scherrer Institut, the Institut Laue-Langevin, and the Forschungsneutronenquelle Heinz Maier-Leibnitz for the allocated beam time. We acknowledge Mark Dean, Maxim Dzero, and Priscila Rosa for fruitful discussions, and Maik Locher for his help with the dc magnetization measurements. We thank the Swiss National Foundation (Grants No. 200021_147071, No. 200021_138018, and No. 200021_157009 and Fellowships No. P2EZP2_175092 and No. P2EZP2_178542) for financial support. This work used resources of the National Synchrotron Light Source II, a U.S. Department of Energy (DOE) Office of Science User Facility operated for the DOE Office of Science by Brookhaven National Laboratory under Contract No. DE-SC0012704.

*daniel.mazzone@psi.ch
†nicolas.gauthier4@gmail.com

[1] N. Doiron-Leyraud, C. Proust, D. LeBoeuf, J. Levallois, J. Bonnemaison, R. Liang, D. A. Bonn, W. N. Hardy, and L. Taillefer, Quantum oscillations and the Fermi surface in an underdoped high-T_c superconductor, Nat. Phys. **447**, 565 (2007).

[2] A. A. Kordyuk, Iron based superconductors: Magnetism, superconductivity, and electronic structure, Low Temp. Phys. **38**, 888 (2012).

[3] N. D. Mathur, F. M. Grosche, S. R. Julian, I. R. Walker, D. M. Freye, R. K. W. Haselwimmer, and G. G. Lonzarich, Magnetically mediated superconductivity in heavy fermion compounds, Nature (London) **394**, 39 (1998).

[4] S. Catalano, M. Gibert, J. Fowlie, J. Iniguez, J.-M. Triscone, and J. Lreisel, Rare earth nickelates $RNiO_3$: Thin films and heterostructures, Rep. Prog. Phys. **81**, 046501 (2018).

[5] S. Friedemann, T. Westerkamp, M. Brando, N. Oeschler, S. Wirth, P. Gegenwart, C. Krellner, C. Geibel, and F. Steglich, Detaching the antiferromagnetic quantum critical point from the Fermi-surface reconstruction in $YbRh_2Si_2$, Nat. Phys. **5**, 465 (2009).

[6] L. Jiao, Y. Chen, Y. Kohama, D. Graf, E. D. Bauer, J. Singleton, J.-X. Zhu, Z. Weng, G. Pang, T. Shang, J. Zhang, H.-O. Lee, T. Park, M. Jaime, J. D. Thompson, F. Steglich, Q. Si, and H. Q. Yuan, Fermi surface reconstruction and multiple quantum phase transitions in the antiferromagnet $CeRhIn_5$, Proc. Natl. Acad. Sci. U.S.A. **112**, 673 (2015).

[7] J. Custers, K.-A. Lorenzer, M. Müller, A. Prokofiev, A. Sidorenko, H. Winkler, A. M. Strydom, Y. Shimura, T. Sakakibara, R. Yu, Q. Si, and S. Paschen, Destruction of the Kondo effect in the cubic heavy-fermion compound $Ce_3Pd_{20}Si_6$, Nat. Mater. **11**, 189 (2012).

[8] P. Aynajian, E. H. da Silva Neto, A. Gyenis, R. E. Baumbach, J. D. Thompson, Z. Fisk, E. D. Bauer, and A. Yazdani, Visualizing heavy fermions emerging in a quantum critical Kondo lattice, Nature (London) **486**, 201 (2012).

[9] Z. F. Weng, M. Smidman, L. Jiao, X. Lu, and H. Q. Yuan, Multiple quantum phase transitions and superconductivity in Ce-based heavy-fermions, Rep. Prog. Phys. **79**, 094503 (2016).

[10] S. Wirth and F. Steglich, Exploring heavy fermions from macroscopic to microscopic length scales, Nat. Rev. Mater. **1**, 16051 (2016).

[11] M. Dzero, J. Xia, V. Falitski, and P. Coleman, Topological Kondo insulators, Annu. Rev. Condens. Matter Phys. **7**, 249 (2016).

[12] C. Petrovic, P. G. Pagliuso, M. F. Hundley, R. Movshovich, J. L. Sarrao, J. D. Thompson, Z. Fisk, and P. Monthoux, Heavy-fermion superconductivity in $CeCoIn_5$ at 2.3 K, J. Phys. Condens. Matter **13**, L337 (2001).

[13] S. Nakatsuji, D. Pines, and Z. Fisk, Two Fluid Description of the Kondo Lattice, Phys. Rev. Lett. **92**, 016401 (2004).

[14] P. Cermak, P. Javorsky, M. Kratochvlova, K. Pajskr, M. Klicpera, B. Ouladdiaf, M.-H. Lemée-Cailleau, J. Rodriguez-Carvajal, and M. Boehm, Magnetic structures of non-cerium analogues of heavy-fermion Ce_2RhIn_8: The case of Nd_2RhIn_8, Dy_2RhIn_8, and Er_2RhIn_8, Phys. Rev. B **89**, 184409 (2014).

[15] S. Chang, P. G. Pagliuso, W. Bao, J. S. Gardner, I. P. Swainson, J. L. Sarrao, and H. Nakotte, Magnetic structure of antiferromagnetic $NdRhIn_5$, Phys. Rev. B **66**, 132417 (2002).

[16] N. Van Hieu, H. Shishido, T. Takeuchi, A. Thamizhavel, H. Nakashima, K. Sugiyama, R. Settai, T. D. Matsuda, Y. Haga, M. Hagiwara, K. Kindo, and Y. Onuki, Unique magnetic properties of $NdRhIn_5$, $TbRhIn_5$, $DyRhIn_5$, and $HoRhIn_5$, J. Phys. Soc. Jpn. **75**, 074708 (2006).

[17] R. Hu, Y. Lee, J. Hudis, V. F. Mitrovic, and C. Petrovic, Composition and field-tuned magnetism and superconductivity in $Nd_{1-x}Ce_xCoIn_5$, Phys. Rev. B **77**, 165129 (2008).

[18] S. Raymond, S. M. Ramos, D. Aoki, G. Knebel, V. P. Mineev, and G. Lapertot, Magnetic order in $Ce_{0.95}Nd_{0.05}CoIn_5$: The Q-phase at zero magnetic field, J. Phys. Soc. Jpn. **83**, 013707 (2014).

[19] D. G. Mazzone, S. Raymond, J. L. Gavilano, E. Ressouche, C. Niedermayer, J. O. Birk, B. Ouladdiaf, G. Bastien, G. Knebel, D. Aoki, G. Lapertot, and M. Kenzelmann, Field-induced magnetic instability within a superconducting condensate, Sci. Adv. **3**, e1602055 (2017).

[20] P. Willmott *et al.*, The materials science beamline upgrade at the swiss light source, J. Synchrotron Radiat. **20**, 667 (2013).

[21] Zs. Revay, R. Kudejova, and K. Kleszcz, In-beam activation analysis facility at MLZ, Garching, Nucl. Instrum. Methods Phys. Res., Sect. A **799**, 114 (2015).

[22] Zs. Revay, Determining elemental composition using prompt gamma activation analysis, Anal. Chem. **81**, 6851 (2009).

[23] J. Rodriguez-Caravajal, Recent advances in magnetic structure determination by neutron powder diffraction, Physica (Amsterdam) **192B**, 55 (1993).

[24] See Supplemental Material at http://link.aps.org/supplemental/10.1103/PhysRevLett.123.097201 for more details on the methods as well as supplementary macroscopic and neutron diffraction results.

[25] Y. Tokiwa, E. D. Bauer, and P. Gegenwart, Gegenwart. Zero-Field Quantum Critical Point in $CeCoIn_5$, Phys. Rev. Lett. **111**, 107003 (2013).

[26] M. P. Allan, F. Massee, D. K. Morr, J. Van Dyke, A. W. Rost, A. P. Mackenzie, A. C. Petrovic, and J. C. Davis, Imaging Cooper pairing of heavy fermions in $CeCoIn_5$, Nat. Phys. **9**, 468 (2013).

[27] H. Kim, M. A. Tanatar, R. Flint, C. Petrovic, Rongwei Hu, B. D. White, I. K. Lum, M. B. Maple, and R. Prozorov, Nodal to Nodeless Superconducting Energy-Gap Structure Change Concomitant with Fermi-Surface Reconstruction in the Heavy-Fermion Compound $CeCoIn_5$, Phys. Rev. Lett. **114**, 027003 (2015).

[28] S. Ohira-Kawamura, H. Kawano-Furukawa, H. Shishido, R. Okazaki, T. Shibauchi, H. Harima, and Y. Matsuda, Neutron diffraction studies on heavy fermion superconducting and antiferromagnetic compounds $CeRh_{1-x}Co_xIn_5$, Phys. Status Solidi (a) **206**, 1076 (2009).

[29] S. Ohira-Kawamura, H. Shishido, A. Yoshida, R. Okazaki, H. Kawano-Furukawa, T. Shibauchi, H. Harima, and Y. Matsuda, Competition between unconventional superconductivity and incommensurate antiferromagnetic order in $CeRh_{1-x}Co_xIn_5$, Phys. Rev. B **76**, 132507 (2007).

[30] M. Yokoyama, N. Oyama, H. Amitsuka, S. Oinuma, I. Kawasaki, K. Tenya, M. Matsuura, K. Hirota, and T. J. Sato, Change of antiferromagnetic structure near a quantum critical point in $CeRh_{1-x}Co_xIn_5$, Phys. Rev. B **77**, 224501 (2008).

[31] T. J. Liu *et al.*, From $(\pi, 0)$ magnetic order to superconductivity with (π, π) magnetic resonance in $Fe_{1.02}Te_{1-x}Se_x$, Nat. Mater. **9**, 718 (2010).

[32] S. Raymond, K. Kaneko, A. Hiess, P. Steffens, and G. Lapertot, Evidence for Three Fluctuation Channels in the Spin Resonance of the Unconventional Superconductor $CeCoIn_5$, Phys. Rev. Lett. **109**, 237210 (2012).

[33] D. G. Mazzone, S. Raymond, J. L. Gavilano, P. Steffens, A. Schneidewind, G. Lapertot, and M. Kenzelmann, Spin Resonance and Magnetic Order in an Unconventional Superconductor, Phys. Rev. Lett. **119**, 187002 (2017).

[34] J. M. Tranquada, Stripes and superconductivity in cuprates, Physica (Amsterdam) **407B**, 1771 (2012).

[35] Y.-F. Yang and D. Pines, Emergence of superconductivity in heavy electron materials, Proc. Natl. Acad. Sci. U.S.A. **111**, 18178 (2014).

[36] Y.-F. Yang, Two-fluid model for heavy electron physics, Rep. Prog. Phys. **79**, 074501 (2016).

[37] K. Haule, C.-H. Yee, and K. Kim, Dynamical mean-field theory within the full-potential methods: Electronic structure of $CeIrIn_5$, $CeCoIn_5$, and $CeRhIn_5$, Phys. Rev. B **81**, 195107 (2010).

[38] T. Willers, Z. Hu, N. Hollmann, P. O. Körner, J. Gegner, T. Burnus, H. Fujiwara, A. Tanaka, D. Schmitz, H. H. Hsieh, H.-J. Lin, C. T. Chen, E. D. Bauer, J. L. Sarrao, E. Goremychkin, M. Koza, L. H. Tjeng, and A. Severing, Crystal-field and Kondo-scale investigations of $CeMIn_5$ (M = Co, Ir, and Rh): A combined x-ray absorption and inelastic neutron scattering study, Phys. Rev. B **81**, 195114 (2010).

[39] T. Willers, F. Strigari, Z. Hu, V. Sessi, N. B. Brookes, E. D. Bauer, J. L. Sarrao, J. D. Thompson, A. Tanaka, S. Wirth, L. H. Tjeng, and A. Severing, Correlation between ground state and orbital anisotropy in heavy fermion materials, Proc. Natl. Acad. Sci. U.S.A. **112**, 2384 (2015).

[40] K. Chen, F. Strigari, M. Sundermann, Z. Hu, Z. Fisk, E. D. Bauer, P. F. S. Rosa, J. L. Sarrao, J. D. Thompson, J. Herrero-Martin, E. Pellegrin, D. Betto, K. Kummer, A. Tanaka, S. Wirth, and A. Severing, Evolution of ground-state wave function in $CeCoIn_5$ upon Cd or Sn doping, Phys. Rev. B **97**, 045134 (2018).

[41] H. Sakai, F. Ronning, J.-X. Zhu, N. Wakeham, H. Yasuoka, Y. Tokunaga, S. Kambe, E. D. Bauer, and J. D. Thompson, Microscopic investigation of electronic inhomogeneity induced by substitutions in a quantum critical metal $CeCoIn_5$, Phys. Rev. B **92**, 121105(R) (2015).

[42] J. Klotz, K. Götze, I. Sheikin, T. Förster, D. Graf, J.-H. Park, E. S. Choi, R. Hu, C. Petrovic, J. Wosnitza, and E. L. Green, Fermi surface reconstruction and dimensional topology change in Nd-doped $CeCoIn_5$, Phys. Rev. B **98**, 081105 (R) (2018).

[43] P. F. S. Rosa, J. Kang, Yongkang Luo, N. Wakeham, E. D. Bauer, F. Ronning, Z. Fisk, R. M. Fernandes, and J. D. Thompson, Competing magnetic orders in the superconducting state of heavy-fermion $CeRhIn_5$, Proc. Natl. Acad. Sci. U.S.A. **114**, 5384 (2017).

[44] J. H. J. Martiny, M. N. Gastiasoro, I. Vekhter, and B. M. Andersen, Impurity-induced antiferromagnetic order in Pauli-limited nodal superconductors: Application to heavy-fermion $CeCoIn_5$, Phys. Rev. B **92**, 224510 (2015).

[45] S.-Z. Lin and J.-X. Zhu, Impurity-induced magnetic droplet in unconventional superconductors near a magnetic instability: Application to Nd-doped $CeCoIn_5$, Phys. Rev. B **96**, 224502 (2017).